REPORT DOCUMENTATION PAGE

Form Approved OMB NO. 0704-0188

The public reporting burden for this collection of information is estimated to average 1 hour per response, including the time for reviewing instructions, searching existing data sources, gathering and maintaining the data needed, and completing and reviewing the collection of information. Send comments regarding this burden estimate or any other aspect of this collection of information, including suggesstions for reducing this burden, to Washington Headquarters Services, Directorate for Information Operations and Reports, 1215 Jefferson Davis Highway, Suite 1204, Arlington VA, 22202-4302. Respondents should be aware that notwithstanding any other provision of law, no person shall be subject to any oenalty for failing to comply with a collection of information if it does not display a currently valid OMB control number.
PLEASE DO NOT RETURN YOUR FORM TO THE ABOVE ADDRESS.

1. REPORT DATE (DD-MM-YYYY)	2. REPORT TYPE	3. DATES COVERED (From - To)
04-06-2015	Final Report	15-Oct-2013 - 14-Jul-2014

4. TITLE AND SUBTITLE
Final Report: Sulfur Doping of InAs

5a. CONTRACT NUMBER
W911NF-13-1-0447

5b. GRANT NUMBER

5c. PROGRAM ELEMENT NUMBER
611102

6. AUTHORS
Seth R. Bank

5d. PROJECT NUMBER

5e. TASK NUMBER

5f. WORK UNIT NUMBER

7. PERFORMING ORGANIZATION NAMES AND ADDRESSES
University of Texas at Austin
101 East 27th Street
Suite 5.300
Austin, TX 78712 -1532

8. PERFORMING ORGANIZATION REPORT NUMBER

9. SPONSORING/MONITORING AGENCY NAME(S) AND ADDRESS (ES)
U.S. Army Research Office
P.O. Box 12211
Research Triangle Park, NC 27709-2211

10. SPONSOR/MONITOR'S ACRONYM(S)
ARO

11. SPONSOR/MONITOR'S REPORT NUMBER(S)
64792-EL-II.1

12. DISTRIBUTION AVAILIBILITY STATEMENT
Approved for Public Release; Distribution Unlimited

13. SUPPLEMENTARY NOTES
The views, opinions and/or findings contained in this report are those of the author(s) and should not contrued as an official Department of the Army position, policy or decision, unless so designated by other documentation.

14. ABSTRACT
We investigated the sulfur doping limits of InAs using ion implantation and rapid thermal annealing for plasmonic applications. Previous studies suggested that higher electron concentrations would be possible using sulfur doping than silicon, which represents the current state-of-the-art dopant. While we achieved near record active electron concentrations with sulfur, we found that dopant diffusion ultimately limited the maximum achievable carrier concentration. A sealed ampoule synthesis setup, which would not be subject to these limitations, was constructed

15. SUBJECT TERMS
Semiconductor doping, plasmonics, ion implantation, rapid thermal annealing, InAs, sulfur

16. SECURITY CLASSIFICATION OF:			17. LIMITATION OF ABSTRACT	15. NUMBER OF PAGES	19a. NAME OF RESPONSIBLE PERSON
a. REPORT	b. ABSTRACT	c. THIS PAGE			Seth Bank
UU	UU	UU	UU		19b. TELEPHONE NUMBER
					512-471-9669

Report Title

Final Report: Sulfur Doping of InAs

ABSTRACT

We investigated the sulfur doping limits of InAs using ion implantation and rapid thermal annealing for plasmonic applications. Previous studies suggested that higher electron concentrations would be possible using sulfur doping than silicon, which represents the current state-of-the-art dopant. While we achieved near record active electron concentrations with sulfur, we found that dopant diffusion ultimately limited the maximum achievable carrier concentration. A sealed ampoule synthesis setup, which would not be subject to these limitations, was constructed for further studies.

Enter List of papers submitted or published that acknowledge ARO support from the start of the project to the date of this printing. List the papers, including journal references, in the following categories:

(a) Papers published in peer-reviewed journals (N/A for none)

Received Paper

TOTAL:

Number of Papers published in peer-reviewed journals:

(b) Papers published in non-peer-reviewed journals (N/A for none)

Received Paper

TOTAL:

Number of Papers published in non peer-reviewed journals:

(c) Presentations

A.K. Rockwell, S.J. Maddox, R. Salas, V. Dasika, and S.R. Bank, "Rapid Thermal Annealing of Ion Implanted InAs:S for Mid-IR Plasmonics," 56th Electronic Materials Conf. (EMC), Santa Barbara, CA, June 2014.

Number of Presentations: 1.00

Non Peer-Reviewed Conference Proceeding publications (other than abstracts):

Received Paper

TOTAL:

Number of Non Peer-Reviewed Conference Proceeding publications (other than abstracts):

Peer-Reviewed Conference Proceeding publications (other than abstracts):

Received Paper

TOTAL:

Number of Peer-Reviewed Conference Proceeding publications (other than abstracts):

(d) Manuscripts

Received Paper

TOTAL:

Number of Manuscripts:

Books

Received Book

TOTAL:

Received Book Chapter

TOTAL:

Patents Submitted

Patents Awarded

Awards

National Science Foundation Graduate Research Fellowship (NSF-GRF), A.K. Rockwell
Best Paper, Electronic Materials Conference, S.J. Maddox

Graduate Students

NAME	PERCENT_SUPPORTED	Discipline
Ann Katherine Rockwell	0.00	
Scott Joseph Maddox	0.00	
FTE Equivalent:	**0.00**	
Total Number:	**2**	

Names of Post Doctorates

NAME	PERCENT_SUPPORTED
FTE Equivalent:	
Total Number:	

Names of Faculty Supported

NAME	PERCENT_SUPPORTED	National Academy Member
Seth R. Bank	0.00	
FTE Equivalent:	**0.00**	
Total Number:	**1**	

Names of Under Graduate students supported

NAME	PERCENT_SUPPORTED
FTE Equivalent:	
Total Number:	

Student Metrics

This section only applies to graduating undergraduates supported by this agreement in this reporting period

The number of undergraduates funded by this agreement who graduated during this period: 0.00

The number of undergraduates funded by this agreement who graduated during this period with a degree in science, mathematics, engineering, or technology fields:...... 0.00

The number of undergraduates funded by your agreement who graduated during this period and will continue to pursue a graduate or Ph.D. degree in science, mathematics, engineering, or technology fields:...... 0.00

Number of graduating undergraduates who achieved a 3.5 GPA to 4.0 (4.0 max scale):...... 0.00

Number of graduating undergraduates funded by a DoD funded Center of Excellence grant for Education, Research and Engineering:...... 0.00

The number of undergraduates funded by your agreement who graduated during this period and intend to work for the Department of Defense 0.00

The number of undergraduates funded by your agreement who graduated during this period and will receive scholarships or fellowships for further studies in science, mathematics, engineering or technology fields:...... 0.00

Names of Personnel receiving masters degrees

NAME

Total Number:

Names of personnel receiving PHDs

NAME

Total Number:

Names of other research staff

NAME	PERCENT_SUPPORTED
FTE Equivalent:	
Total Number:	

Sub Contractors (DD882)

Inventions (DD882)

Scientific Progress

See Attachment

Technology Transfer

N/A.

STIR: Sulfur Doping of InAs

Seth R. Bank
The University of Texas at Austin

1. Overview

There is a great need to develop nanophotonic components in the mid infrared, ~3-5 µm, for a number of applications in gas sensing, 3-D laser radar, and free-space/integrated data links at the various atmospheric transmission windows, in particular those between ~3-4 µm. Plasmonics offer the prospect of significant device scaling to reduce SWaP and increase integration density for systems, as well as for enhancing device performance and potentially realizing fundamentally new functionality.

As a motivating example, consider the enhancement in spontaneous emission rate that could be achieved by coupling emitters with a nanoscale parallel plate metal waveguide, described in **Figure 1** [1]. Calculations shown in **Figure 1a** indicate that the emission rate can be increased by >90x. Assuming a reasonable radiative lifetime, 1 ns, this corresponds to a modulation rate of ~90 GHz, already beyond what can be typically achieved with direct modulation of vertical-cavity surface-emitting lasers (VCSEL) [2], with greater enhancements being expected with decreasing plate spacing [3].

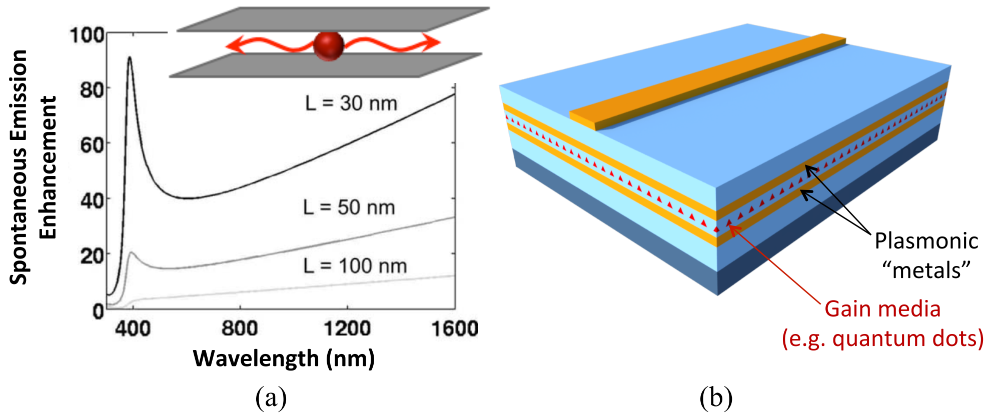

Figure 1. Motivating example for epitaxial plasmonic materials. (a) Calculated enhancement of spontaneous emission rates from a dipole emitter sandwiched between two metal plates, for several plate separations, L. Reproduced from Ref. [1]. (b) Epitaxial implementation of such a structure using doped semiconductors for the “metals” and epitaxial quantum dots for the dipole emitter.

2. Conventional limits of doped semiconductors as “metals”

The plasma frequency, ω_p, is essentially the highest optical frequency that a material will respond to like a metal (i.e. with a free electron plasma). To first order, ω_p is given by:

$$\omega_p \approx \sqrt{\frac{Ne^2}{m^* \varepsilon_0 n_{0,InAs}^2}}$$

where N is the active electron concentration, e is the fundamental charge, m^* is the electron effective mass, ε_0 is the permittivity of free space, and $n_{0,InAs}$ is the refractive index. Increasing the plasma frequency is straightforward to accomplish with increasing (active) doping, N.

The achievable electron concentration is limited by a combination of factors, principally: (1) loss of dopant activation through formation of defect complexes and amphoteric incorporation, (2) degradation of surface morphology, and (3) limits to the achievable flux of dopant atoms during the growth. We have found significant benefits towards (1) and (2) by growing at low temperatures, near stoichiometry, and using bismuth as a surfactant to maintain smooth morphology [4] and increase dopant activation beyond the conventional limits [5]. However, the activation of silicon is currently $\sim 1\times10^{20}$ cm^{-3}, which limits the wavelength equivalent to the plasma frequency to >4 μm.

Glazov and co-workers studied several alternative n-type dopants (sulfur, selenium, and tellurium) for InAs using direct fusion in a sealed ampoule, in concert with annealing and quenching steps [6]. Their key result is reproduced **Figure 2**, which plots the electron concentration versus sulfur concentration, the species that produced the highest active electron concentrations of any of the dopants studied. Significantly higher electron concentrations were achieved with sulfur, with close to unity dopant activation $>7\times10^{20}$ cm^{-3}, close to what is required to build devices operating at 5 μm. This is a very promising avenue to pursue, particularly if higher doping concentrations can be achieved with modern kinetically-limited synthesis techniques.

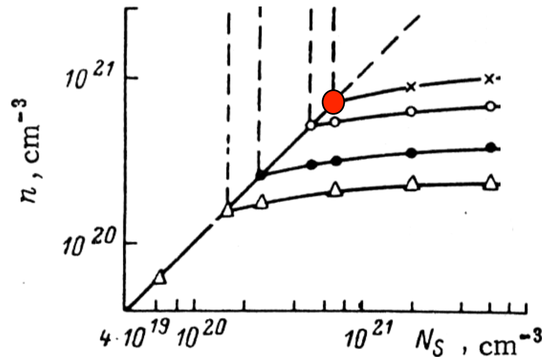

Figure 2. Electron concentration versus sulfur concentration for several annealing temperatures, 900°C (×), 850°C (o), 800°C (•), and 700°C (Δ), which were each followed by rapid quenching. Adapted from Ref. [6]. Note that the maximum achievable electron concentration increased significantly with annealing temperature and activation was nearly unity up to 7.2×10^{20} cm^{-3} (red dot), significantly higher than that achieved with silicon.

3. Technical approach

Unfortunately, sulfur has seen only limited use as a dopant in III-V molecular beam epitaxial (MBE) growth, due to the high vapor pressure. This is a significant concern as high vapor pressure species cause memory effects where layers grown subsequently are unintentionally doped. While this could be mitigated in the future, for example using a cluster MBE where sulfur doping and active (undoped) layers are grown in separate chambers, such a significant capital investment is not reasonable at this preliminary stage. Our focus was to employ ion implantation and rapid thermal annealing (RTA) to gauge the potential utility of sulfur as a dopant for plasmonic applications. Ion implantation is an attractive alternative to sealed ampoule synthesis as it (1) is commercially available, (2) does not require the long (17-50 day) annealing steps associated with powder synthesis [6], and (3) yields the smooth surfaces that are essential for characterizing the plasma frequency with optical reflectivity and surface plasmon propagation with attenuated total reflectance.

4. Experimental design

4.1 Implantation

Each experiment began with the MBE growth of a 200 nm layer of undoped InAs on 3-inch diameter semi-insulating GaAs wafers. Wafers were then ion-implanted with varying sulfur doses at peak concentration depths of 50 nm, providing ~100 nm of sulfur-doped InAs. This was thin enough to

remain achievable by singly-ionized ion implantation, yet thick enough for accurate determination of the active carrier concentration and plasma wavelength by Hall effect and reflectivity measurements.

Implanted wafers were then cleaved into several smaller samples for a systematic activation-annealing temperature study, which was performed in a rapid thermal annealing (RTA) furnace. Rapid thermal annealing was chosen to mitigate sulfur diffusion to maximize the peak carrier concentration. Surface capping was employed to prevent undesirable arsenic out-diffusion during annealing, which can result in defective material and limit dopant activation.

Samples were then thoroughly characterized with Hall Effect (carrier concentration and mobility), optical reflectivity (plasma frequency), and secondary ion mass spectrometry (sulfur depth profiling).

4.2 Implantation conditions

As discussed in the following subsections, the ion implantation conditions were carefully designed to maximize sulfur activation, concentrating on (1) maintaining stoichiometry at these high doping levels, (2) maintaining abrupt doping profiles for maximum carrier densities, and (3) maximizing dopant activation.

4.2.1 Co-implantation to maintain stoichiometry

When implanting compound semiconductors at high doses, it is essential to co-implant additional matrix material to maintain stoichiometry and increase activation after annealing. This is illustrated by two studies summarized in **Figure 3**, where co-implantation of the group-V element was employed to compensate for the additional dopant atoms that sit on the group-III sublattice [7], [8]. Increased doping activation occurred without penalty to the electrical properties (e.g. Ref. 9). Similar results were also observed with co-implantation of gallium with selenium, which sits on the group-V site [10]. Consequently, the sulfur dose was matched with an equal implant dose of indium to maintain stoichiometry and maximize doping activation [9], [11].

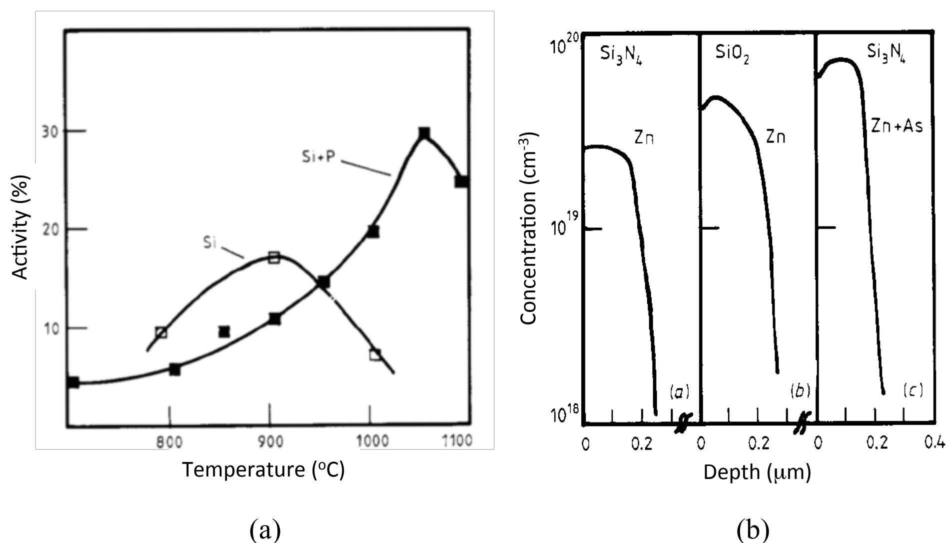

(a) (b)

Figure 3. Benefits of co-implantation of group-V and dopant. (a) Electrical activity versus annealing temperature for implantation with silicon only and co-implantation of silicon and phosphorus [8]. Note the significant enhancement in dopant activation with co-implantation. (b) Depth profiles of active carrier concentration, for Zn-doped GaAs [7]. Note the importance of the capping layer (comparing left and middle curves) and the benefits of co-implantation with arsenic (comparing left and right curves).

4.2.2 Substrate heating during ion implantation

Due to the high implant dosages required, implants were performed at elevated substrate temperature to prevent amorphization [12]. However, the maximum implantation temperature is limited by the onset of group-V desorption, which would compromise stoichiometry. As seen in **Figure 4**, the critical temperature necessary prevent amorphization of the InAs is expected to close to room temperature [13]. All implants were performed at a substrate temperature of 300°C (573 K), which was expected to be well above the critical temperature necessary to prevent amorphization, as seen in **Figure 4** [13], though sufficiently low to avoid group-V desorption during implantation. Desorption and amorphization were not found to be issues implanting at 300°C.

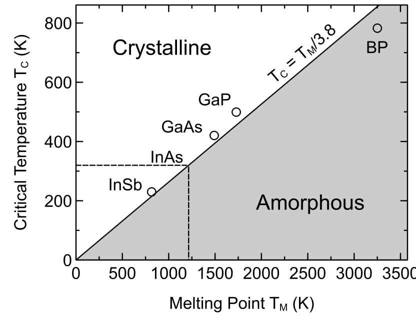

Figure 4. Critical substrate temperature for a given total implant energy, below which amorphization occurs, as a function of the material melting point. The solid line represents a linear fit to the data. Using the melting point for InAs, 1215 K, we estimate a critical temperature of ~50°C (~320 K) (dashed lines). Data from Ref. [13].

4.2.3 Surface protection during rapid thermal annealing

The surface had to be capped after implantation to prevent sublimation of the group-V species during RTA. Comparing the depth profiles in **Figure 3b**, it is clear that the choice of capping material is critical for achieving dopant activation. A GaAs proximity cap was initially chosen to prevent undesirable arsenic out-diffusion during annealing, which can result in defective material and limit dopant activation. More advanced proximity caps, such as PECVD-deposited SiO_2 or Si_3N_4 [7], proved to be necessary to maintain smooth surface morphology.

5. Results

We concentrated on two implantation doses of 1×10^{15} and 3×10^{15} cm^{-2} sulfur atoms, resulting in (expected) average sulfur-doping concentrations of $\sim1\times10^{20}$ and 3×10^{20} cm^{-3}, respectively, in the top ~100 nm of InAs. The lower dose served as a comparison to the highest active carrier concentration we have achieved in MBE-grown silicon-doped InAs (9.6×10^{19} cm^{-3}) at that time, while the higher dose was intended to determine whether we could achieve higher doping concentrations with sulfur.

5.1 Surface morphology and alternative capping methods

Our initial efforts were hampered by poor surface morphology, as readily seen in Nomarski phase contrast imaging. As shown in **Figure 5a**, the surface morphology was quite poor using a proximity cap during RTA. The post-RTA surface morphology improved dramatically with a SiN_x capping layer, as illustrated by **Figure 5b**.

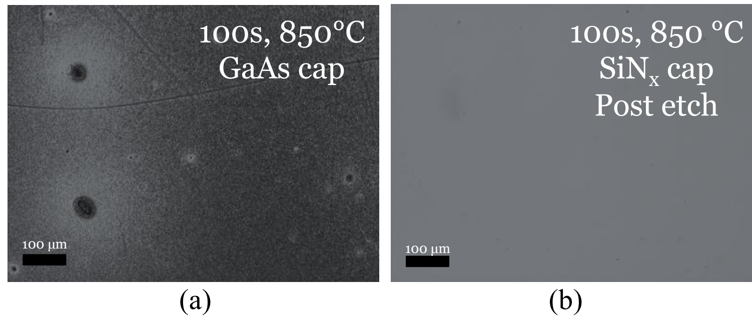

(a) (b)

Figure 5. Nomarski phase contrast microscope images after a 100s RTA at 850°C using a (a) GaAs proximity cap and (b) a PECVD-deposited SiN_x cap after selectively removing the SiN_x with HF:H_20 (1:50). Note the dramatic improvement in surface morphology with the SiN_x cap.

5.2 Electrical properties

We investigated the electrical properties using four-point probing, initially using only proximity capping. As summarized in **Figure 6a**, the sheet concentration was not particularly sensitive to the annealing temperature chosen. Under the assumption that the sulfur was confined within the InAs layer, the percent sulfur activation was calculated from the sheet concentration (**Figure 6b**), assuming electron mobilities measured for InAs doped with silicon, which we have extensively studied. The lower dose, 1×10^{15} cm^{-2}, appeared to yield reasonably high activations. While the higher dose, 3×10^{15} cm^{-2}, exhibited lower activation, the results suggested that the overall carrier concentration increased with the dose, which was promising.

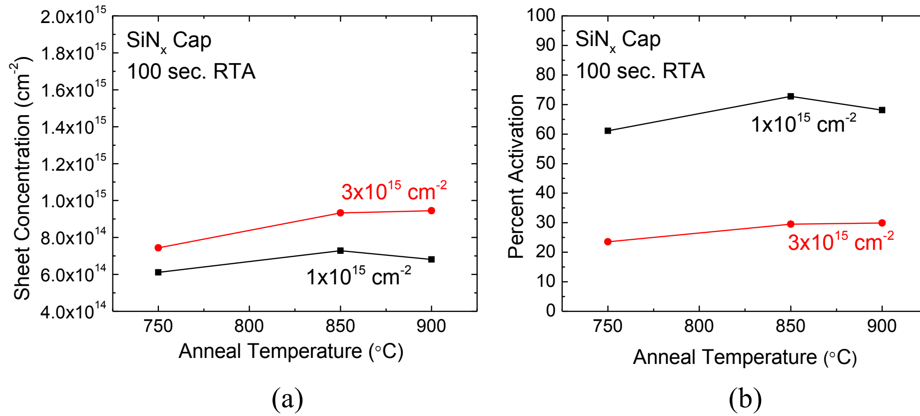

(a) (b)

Figure 6. Annealing dependence of (a) sheet carrier concentration and (b) percent activation, for implantation doses of 1×10^{15} and 3.16×10^{15} cm^{-2} sulfur atoms.

We suspected that the relatively low activations – as well as the insensitivity to annealing temperature – could have been caused by issues related to the capping, based upon the findings detailed in **Section 5.1**. Therefore, we performed Hall Effect measurements, comparing proximity-capped samples with those capped with SiN_x. The results are summarized in **Figure 7**. We found a dramatic reduction in the sheet carrier concentration, as well as a significant increase in electron mobility. Though not unexpected, this was quite promising. We believe that the surface degradation evident in the proximity-capped samples (**Figure 5a**) caused increased sulfur diffusion into the undamaged GaAs, which increased the sheet concentration and decreased the mobility. Employing the SiN_x cap mitigated these effects, improving both the sheet concentration and electron mobility.

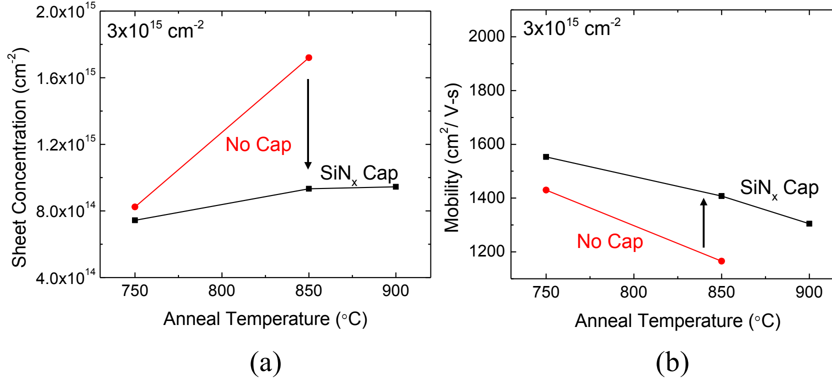

Figure 7. Annealing dependence of (a) sheet carrier concentration and (b) electron mobility, for implantation doses of 1×10^{15} and 3.16×10^{15} cm^{-2} sulfur atoms.

5.3 Optical properties

Optical reflectivity was performed with a Fourier transform infrared (FTIR) spectrometer on the samples; representative results are plotted in **Figure 8**, along with a high-quality MBE-grown silicon-doped InAs sample for reference. Due to the thinner layers, which were limited by the constraints of ion implantation (**Section 4.1**), the InAs:S samples did not exhibit as well-defined a Drude edge in reflectivity as the thicker InAs:Si samples. Surprisingly, the plasma frequencies were unexpectedly low in the sulfur-doped samples, inconsistent with the calculations using the measured sheet concentrations and mobilities.

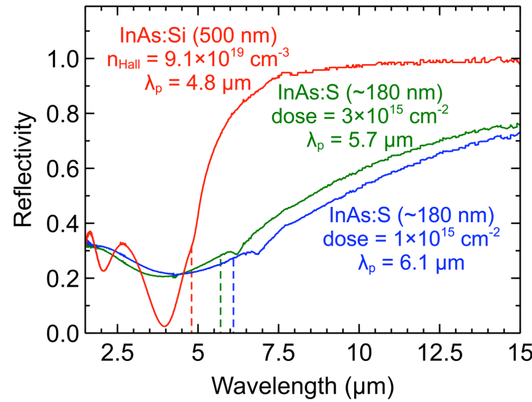

Figure 8. Optical reflectivity of InAs:S samples with implantation doses of 1×10^{15} and 3.16×10^{15} cm^{-2} sulfur atoms, compared with a reference InAs:Si. As expected, the implanted structures exhibited a more gradual Drude edge, which was attributed to the thinner doped regions; however, the measured plasma frequencies were significantly lower than expected from the Hall Effect data.

5.4 Depth profiling

To understand why the plasma frequencies were lower than anticipated in the sulfur-doped samples, we performed SIMS measurements on an as-implanted (**Figure 9a**) and a representative annealed (**Figure 9b**) sample. These results unambiguously point to sulfur diffusion as the culprit for the low plasma frequencies measured with optical reflectivity, despite using RTA to mitigate diffusion. Sulfur diffusion reduced the peak carrier concentration, decreasing the plasma frequency.

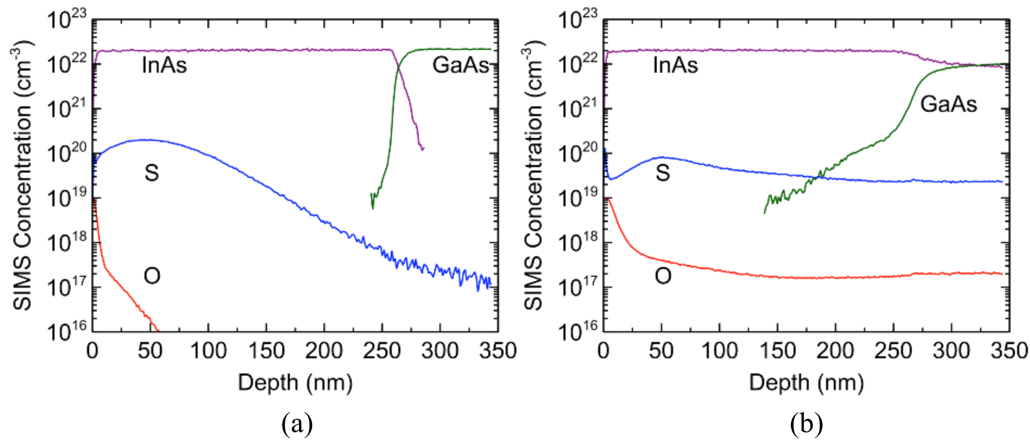

Figure 9. SIMS measurements of (a) as-implanted and (b) annealed structures. Note the dramatic diffusion of sulfur (blue curve), despite using RTA processing to mitigate diffusion.

6. Conclusions and current-state

We determined that the issues with sulfur diffusion evident in the SIMS results in **Figure 9**, were unavoidable; even with shorter and lower temperature annealing, we were unable to obtain Drude edges in reflectivity that matched with the electrical properties. Upon consultation with the program manager, we reallocated the remainder of funds to build a sealed ampoule furnace to replicate the findings of Glasov *et al.* directly. We acquired a working three-zone furnace and purchased the necessary equipment to tool it for InAs:S synthesis. This work is currently in progress.

7. References

---

[1] Y. C. Jun, R. D. Kekatpure, J. S. White, and M. L. Brongersma, “Nonresonant enhancement of spontaneous emission in metal-dielectric-metal plasmon waveguide structures,” *Phys. Rev. B*, vol. 78, pp. 153111-1-4, Oct. 2008.

[2] For example, D. M. Kuchta *et al.*, “A 56.1Gb/s NRZ Modulated 850nm VCSEL-Based Optical Link,” *Optical Fiber Conference (OFC)*, Anaheim, CA, Mar. 2013.

[3] Modification to the optical density of states and increase in the optical intensity in the waveguide should increase with decreasing plate spacing, so the spontaneous emission should increase in proportion, provided that electronic pathways for relaxation (e.g. tunneling of carriers into the metal plates) do not become too severe. From prior studies, enhanced non-radiative pathways become severe at emitter/metal spacings of ~10 nm.

[4] S.J. Maddox, A.P. Vasudev, V.D. Dasika, M.L. Brongersma, and S.R. Bank, "Bismuth Surfactant-Mediated Epitaxy of Highly Doped InAs for Mid-Infrared Plasmonics," *North American Molecular Beam Epitaxy Conf. (NAMBE)*, Stone Mountain Park, GA, Oct. 2012.

[5] S. Law, D.C. Adams, A.M. Taylor, and D. Wasserman, “Mid-infrared designer metals,” *Optics Express*, vol. 20, pp. 12155-12165, May 2012.

[6] V. M. Glazov, R. A. Akopyan, and E. I. Shvedkov, “Investigation of the relationship between the electron density and solubilities of sulfur, selenium, and tellurium in indium arsenide,” *Sov. Phys. Semicond.*, vol. 10, no. 4, pp. 378–380, Apr. 1976.

[7] D. E. Davies, “Transient thermal annealing in GaAs,” *Nucl. Instrum. Meth. B*, vol. 7/8, pp. 387-394, 1985.

[8] C. W. Farley, T. S. Kim, B. G. Streetman, “Co-Implantation and autocompensation in close contact rapid thermal annealing of Si-implanted GaAs:Cr,” *J. Electron. Mater.*, vol. 16, pp. 79-85, 1987.

[9] K. K. Patel and B. J. Sealy, “Rapid thermal annealing of Mg^{+}+As^{+} dual implants in GaAs,” *Appl. Phys. Lett.*, vol. 48, pp. 1467-1469, 1986.
[10] T. Ambridge, R. Heckingbottom, E. C. Bell, B. J. Sealy, K. G. Stephens, and R. K Surridge, “Effect of dual implants into GaAs,” *Electron. Lett.*, vol. 11, pp. 314-315, July 1975.
[11] B. J. Sealy, “Rapid thermal annealing of ion-implanted GaAs,” *Semicond. Sci. Technol.*, vol. 3, no. 5, p. 448, May 1988.
[12] J.S. Harris, F.H. Eisen, B. Welch, J.D. Haskell, R.D. Pashley, and J.W. Mayer, “Influence of implantation temperature and surface protection on tellurium implantation in GaAs,” *Appl. Phys. Lett.*, vol. 21, pp. 601-603, Dec. 1972.
[13] K. Gamo, M. Takai, H. Yagita, N. Takada, K. Masuda, S. Namba, and A. Mizobuchi, “Implantation temperature for III–V compound semiconductors,” *J. Vac. Sci. Technol.*, vol. 15, no. 3, pp. 1086–1088, 1978.